Micro-Raman spectroscopy of refractive index microstructures in silicone-based hydrogel polymers created by high-repetition-rate femtosecond laser micromachining

Li Ding,[1,*] Luiz Gustavo Cancado,[1] Lukas Novotny,[1] Wayne H. Knox,[1] Neil Anderson,[2] Dharmendra Jani,[2] Jeffrey Linhardt,[2] Richard I. Blackwell,[2] and Jay F. Künzler[2]

[1]*The Institute of Optics, University of Rochester, Rochester, New York 14627, USA*
[2]*Bausch and Lomb, 1400 North Goodman Street, P.O. Box 30450, Rochester, New York 14603, USA*
[*]*Corresponding author: dingli@optics.rochester.edu*

Received October 21, 2008; accepted January 8, 2009;
posted January 26, 2009 (Doc. ID 102944); published March 3, 2009

Micro-Raman spectroscopy was used to study silicone-based hydrogel polymers after being modified by 800 nm, 27 fs laser pulses from a Ti:sapphire oscillator at 93 MHz repetition rate. When the irradiation conditions were below the optical breakdown threshold of the polymers, no significant changes in the Raman spectra and background fluorescence were observed even when refractive index changes as large as $+0.06\pm0.005$ were observed. On the other hand, changes in the Raman spectra and fluorescence were easily detected when higher pulse energy was employed to induce visible optical damage in the hydrogel polymers. These results show that a significant refractive index modification, below the optical breakdown threshold in silicone-based hydrogel polymers, can be realized in the absence of any significant change in the Raman spectrum of polymer composition. A thermal model is presented to explain these results. It shows that high-repetition-rate laser pulses cause significant heat accumulation, which can induce additional cross-linking and densification in the polymer network, resulting in locally increased refractive index.

OCIS codes: 160.5470, 300.6450, 320.2250.

1. INTRODUCTION

Recently, near-infrared femtosecond lasers have been used to create different structures in many transparent optical materials including silica glasses [1–9] and various polymers [10–17]. In the present study, femtosecond laser pulses are tightly focused inside transparent hydrogel polymer materials through a high (or medium) numerical aperture (NA) objective. In the course of the femtosecond laser micromachining process, the energy transfer rate achieved in the induced nonlinear absorption is much higher than the rate at which it can be dissipated into the surrounding lattice. This process allows a strongly localized energy deposition in the focal volume. Due to the high laser intensity within the focal volume, the nonlinear absorption can create a microplasma, which leads to a range of local material modifications, leaving the surrounding medium unaffected. Since this special material modification does not involve photolithography, it provides femtosecond laser micromachining a unique 3D manufacturing capability on different optical transparent materials.

Many research groups have reported the use of femtosecond laser pulses to manufacture optical waveguides, couplers [1–6,13,17], 3D storages [7], optical gratings [10], photonic crystals [15], and microfluidic channels [8,9,16]. Although different experimental conditions (e.g., laser pulse energy and width, scanning speed, repetition rate, etc.) are employed in different experiments, the results achieved can be classified into two main categories depending on whether they can induce optical breakdown in the irradiated materials or not. In the absence of optical breakdown, the femtosecond laser-induced modifications will be relatively small. In this case, only the refractive index may be changed and this property can be used to create refractive or diffractive components such as waveguides and gratings. Refractive index changes in the range of 1×10^{-2} to 1×10^{-4} in ordinary silica glasses (without doping) and poly(methyl methacrylate) (PMMA) polymers have been widely observed [1,2,4,5,13,14,17]. However, if the irradiation parameters are strong enough to cause optical breakdown, microexplosions followed by visible plasma luminescence and shock waves will be created inside of the medium. Such a process will induce significant structural and morphological modifications in the material, causing optical damage. Optical 3D storages, photonic crystals, and microfluidic channels directly fabricated by the femtosecond laser pulses are usually in this category, and additional procedures and a special experimental environment are sometimes needed to yield these results [7–9,15,16].

We recently reported that large refractive index changes (in the range of 0.03 to 0.06) could be induced in three different biocompatible hydrogel polymers by megahertz repetition-rate, nanojoule pulse-energy femtosecond laser pulses [10]. The three hydrogel polymers used were HEMA (2-hydroxyethyl methacrylate), RD1817 (a copolymer of 2-hydroxyethyl methacrylate and N-1-vinyl-pyrrolidinone), and PV2526 or Balafilcon A [tris(trimeth-

ylsiloxy)silyl propylvinyl carbamate (TPVC), *N*-vinyl pyrrolidone (NVP), and other silicone components] [18]. These hydrogel polymers contain 36% to 80% of water and have been widely used in the contact lens industry because of their high optical clarity and high water and oxygen permeability. Since a 93 MHz laser pulse train was employed to induce the refractive index changes in these hydrogel polymers, heat accumulation within the focal volume during the experiments must be considered. Different from low-repetition-rate (10 Hz to 1 MHz) femtosecond laser pulse trains, high-repetition-rate (>10 MHz) femtosecond laser pulse trains have a much shorter time interval between adjacent pulses, which may be even less than the heat diffusion time within the material. As a result the nonlinear absorbed laser energy will accumulate within the focal volume, increasing the temperature inside and near the laser–material interaction region, eventually inducing modifications [6,19,20]. Since these special hydrogel polymers are composed of water-swollen polymer networks, water also plays an important role in the femtosecond laser-induced modifications [21,22]. Furthermore, it may also have been noticed that the low density plasma generation below the optical breakdown threshold in water may induce thermoelastic stress and stress-induced bubbles, which will affect the laser-induced modifications even if no visible plasma luminescence is observed [21]. Therefore, the combined effects of several different experimental factors may eventually cause the large refractive index changes within these special hydrogel polymers induced by high-repetition-rate and low-pulse-energy femtosecond laser pulses.

Due to its high sensitivity to structural changes, Raman spectroscopy has been used to analyze materials irradiated by femtosecond laser pulses, such as fused silica glass [20,23–25], doped glass [26–28], silicon wafers [29,30], and As_2S_3 thin film [31]. In this paper, we present our further investigations on the femtosecond laser induced modifications in hydrogel polymers by employing Raman spectroscopic method. Unlike the results reported for fused glass [20,23–25], our results show that the refractive index modification below the optical breakdown threshold in silicone-based hydrogel polymers is not accompanied by significant change in the Raman spectrum. The accumulated effects of the femtosecond pulses can induce additional cross-linking of the polymer network, causing expulsion of water, localized densification, and a concomitant increase in the local refractive index.

2. EXPERIMENTAL METHOD AND MATERIAL PREPARATION

The hydrogel polymer used in this work was the Balafilcon A from Bausch and Lomb [10], which has been widely used in order to make the fifth and most recent generation of hydrogel contact lenses. The polymer is derived from TPVC, NVP, and other silicone components [18]. Cross-linking polymer components are normally present in these hydrogels at a level of less than 1% by weight. Figure 1 shows the structures of the two principal monomers (TPVC and NVP) that are incorporated in Balafilcon A. Bonds present in the hydrogel polymer and evident in the Raman spectrum are -Si-$(CH_3)_x$, -Si-O-Si-, -Si-O_3, and

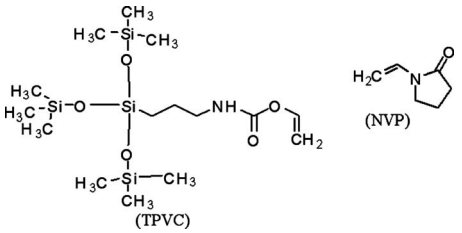

Fig. 1. Molecular structures of two major monomers polymerized in Balafilcon A, the TPVC (left-hand side) and NVP (right-hand side)

-CH_x. Urethane and pyrrolidone carbonyl stretching frequencies evidently are not Raman active, or they may be present levels that are below our detection sensitivity. The Balaficon A bulk contains 36% water by weight and has an average refractive index of 1.4220 [10]. Using an Ocean Optics HR4000 spectrometer we have found the cutoff wavelength of its transmission spectra within the range of 300 to 350 nm, and the material is transparent near 800 nm [10].

The femtosecond laser apparatus used to modify the hydrogel polymers is similar as the one described in [10]. The laser source was a Kerr-lens mode-locked Ti:sapphire femtosecond laser oscillator (K-M Labs), generating pulses of 300 mW average power, 27 fs pulsewidth, and 93 MHz repetition rate at 800 nm. Two SF10 prisms in a double-pass configuration were used to compensate the significant dispersion induced by a large amount of glass in the focusing objective. The femtosecond laser pulses were focused into the hydrogels using a 60× 0.70 NA Olympus LUCPlanFLN long-working-distance objective that could precisely correct the spherical aberration introduced by refractive index mismatch between the coverslip and hydrogel polymers and created a nearly diffraction-limited laser focus. Throughout the whole experimental process the hydrogel samples were mounted in a borate buffered saline (BBS) solution between two cover glass slides, maintaining their water content. A 3D scanning platform formed by three Newport VP-25XA linear servo stages with 100 nm resolution was employed to move the hydrogel samples transversely to the direction of the laser beam. In addition, a charge coupled device (CCD) camera was mounted beside the samples to monitor the modification process.

Raman scattering measurements were performed at room temperature using a 3 mW HeNe laser source with wavelength of 632.8 nm. The experimental Raman setup is based on an inverted optical microscope with an $x-y$ scan stage. The linearly polarized incident laser beam is reflected by a dichroic beam splitter and focused by a high NA oil immersion objective (1.4 NA) on the sample surface through the transparent glass substrate. The scattered light is collected with the same objective and is detected in two distinct ways. In the first, the scattered beam is transmitted through the beam splitter and filtered by a bandpass filter in order to remove all the scattered light with wavelength outside of the range in which the Raman band to be studied is centered on. Then, the filtered scattered beam is detected by a single-photon counting avalanche photodiode (APD). In the second option, the scattered beam is transmitted through the beam

splitter and filtered by a notch filter in order to remove the Rayleigh component of the scattered light. The signal is then detected by a combination of a spectrograph and a cooled CCD.

3. RESULTS

Figure 2(a) shows 40 μm long smooth lines fabricated at the hydrogel surface using a differential interference contrast (DIC) microscopic mode. 1.3 nJ pulse energy below the optical breakdown threshold was initially used to create 0.06 refractive index change along the lines in the femtosecond laser fabrication process. Using the same knife edge method as reported in our previous experiments [10], we measured a laser focal diameter of about 2.5 μm. This focal diameter gave raise to laser-irradiated lines of approximately 1 μm wide and 3 μm deep. Long-term maintenance of these refractive index modifications was checked, showing that the modifications were permanently induced in the Balafilcon A hydrogels.

Figure 2(b) shows the confocal luminescence image of the region shown in Fig. 2(a). The image was obtained by placing a 700 nm bandpass filter (10 nm width) in front of the APD, allowing light within this spectral window (695–705 nm) to be detected. The laser-induced refractive index changes lead to a lensing effect, which gives rise to bright features in the confocal luminescence image. These features correspond to the machined lines. We maximized the confocal signal by centering, in three dimensions, the laser focus into the modified region and then acquired Raman spectra.

Raman spectra were also acquired in the BBS solution under the same conditions (60 s of acquisition time).

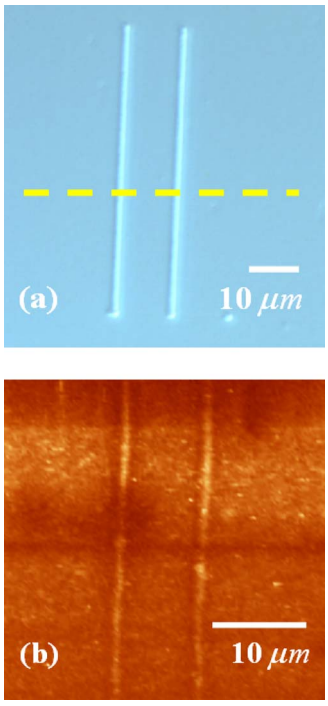

Fig. 2. (Color online) (a) DIC image of laser modified lines on the surface of Balafilcon A. Several Raman spectra were taken along the dashed line. (b) Confocal luminescence image of these lines (the wavelength detection window is 695–705 nm).

These spectra define the reference for the baseline profile. A representative reference spectrum is shown in Fig. 3. It features a broad fluorescence band without any obvious Raman peaks.

To detect any structural modifications in the machined region, several Raman spectra were taken along the dashed line shown in Fig. 2(a). In this process, the HeNe laser focal point was moved in 400 nm steps. Since the confocal lateral resolution of the HeNe laser focal volume is about 250 nm, both Raman spectra of the bulk and laser-modified region were confirmatively taken during the measurement.

Figures 4(a) and 4(b) show the original Raman spectra of the bulk and machined regions of Balafilcon A hydrogel taken in the experiments. In both spectra several Raman peaks were detected over the broad fluorescence background. Fluorescence background difference was first checked between the two spectra. It is known that material defects generated by the megahertz femtosecond laser pulses increase background fluorescence intensity in fused silica [25]. In the case of polymers, monomers, or other molecule fragments resulting from degradation of the polymer network or backbone can also increase the background fluorescence intensity either in the pyrolytic decomposition process or in the UV laser ablation process [32,33]. Here, no significant change of fluorescence background was detected, indicating that the femtosecond laser machining process did not produce a large number of defects, monomers, or molecule fragments in the hydrogel. The Raman signal was then checked by subtracting the fluorescence background from the original spectra. Figure 4(c) shows the Raman spectra of the bulk Balafilcon A hydrogel in BBS solution after baseline correction. We assigned the Raman peaks to various material bonds (see Table 1) [34,35]. Urethane and pyrrolidone carbonyl stretching frequencies evidently are not Raman active, or they may be present at levels that are below our detection sensitivity. Figure 4(d) shows the Raman spectra of the femtosecond laser-modified refractive index change lines in PureVision™ (PV) hydrogel shown in Fig. 2, obtained under the same conditions as the spectra shown in Fig. 4(c). As shown in Fig. 4, the Raman spectra obtained from the machined region is similar to the Raman spectrum obtained from the bulk, since no significant difference is detected. Even the intensity ratio between different Raman

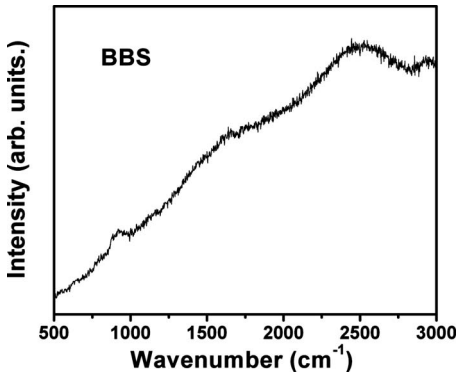

Fig. 3. One typical Raman spectrum of BBS solution indicates a broad fluorescence band without any obvious Raman peaks within the spectrum region from 500 to 3000 cm^{-1}.

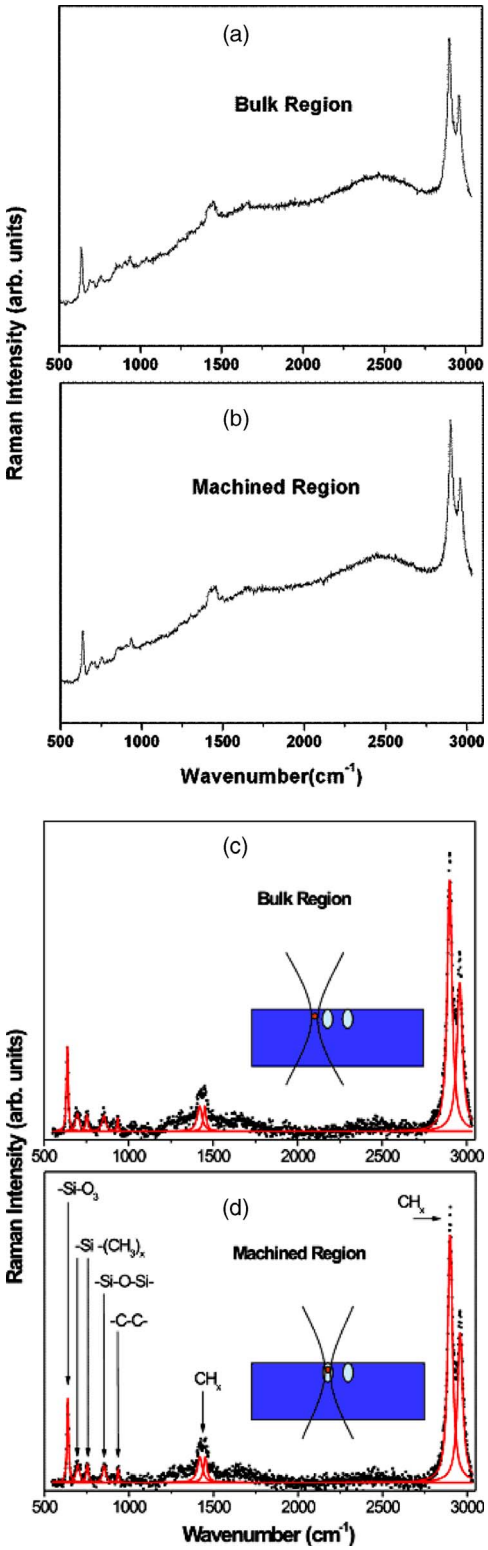

Fig. 4. (Color online) (a) Raman spectra of the bulk Balafilcon A hydrogel in BBS solution with fluorescence background. (b) Raman spectra of the femtosecond laser modified refractive-index-change region with fluorescence background. (c) Raman spectra of the bulk region with baseline correction (removal of broad features), the inset is the cross section of the two modified lines in hydrogel while the confocal focus for the Raman signal measurement locates in the bulk. (d) Raman spectra of the machined region with background correction, the inset shows the confocal laser focus locates inside the machined line to detect its Raman spectra.

Table 1. Raman Assignments for the PV (Balafilcon A) Hydrogel [34,35]

Assignment	Wavenumber (cm^{-1})
-CH_X stretching	2890/2958
-CH_X deformation	1418
C-C skeletal	935
-Si-O-S- stretching	852
-Si-$(CH_3)_X$ stretching	686–752
-Si-O_3 stretching	638

peaks remains unchanged. We observed that no detectable change in the Raman spectrum occurs for any size refractive index modification below the damage threshold.

Figure 5 shows a bright field image of a laser-damage spot in PV hydrogel obtained by increasing the laser irradiance to 800 mW average power. Visible plasma luminescence was clearly observed during the process. This optical breakdown region was deliberately induced in order to see if the Raman spectrum would change in the case of damage. As shown in Fig. 5, although the initial dimension of the femtosecond laser focal volume did not change, the size of the damage spot was significantly larger than the laser spot because of the significant heat dissipation and water bubble cavitation expansion from the laser focus [21,22]. Black residue was formed primarily in the epicenter of the spot.

Significant nonuniformity of the Raman spectrum near the laser-affected regions inside the damage spot can be observed. Figure 6 shows the Raman spectra of different measured points of the damage spot from its periphery (point 1) to its center (point 4). The acquisition times for Figs. 6(a)–6(d) and Fig. 6(d) were 60 and 10 s, respectively. Figure 6(a) is the Raman spectra of the most outside region (point 1) of the damage spot in Fig. 5 where the accumulated heat diffused from the center of the damage spot and affected this region. Although the intensities and positions of the Raman peaks were maintained, a broad fluorescence band centered at 1500 cm^{-1} was observed. This broad fluorescence was not been seen in Figs. 4(a) and 4(b). Comparing Figs. 6(b) and 6(c), which show the Raman spectra of points 2 and 3 that are closer to the center of the damage spot, the intensity of the broad fluorescence band increases and ultimately becomes so large

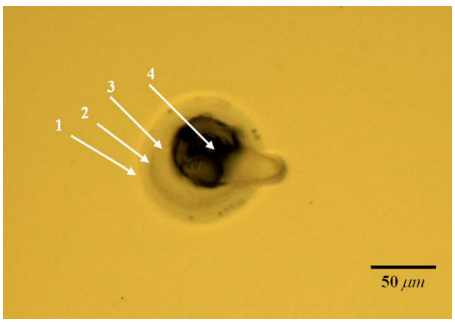

Fig. 5. (Color online) Bright field image of a damage spot in Balafilcon A with high femtosecond laser irradiance. Raman spectra of four points of the damage spot from its periphery (point 1) to its center (point 4) were measured.

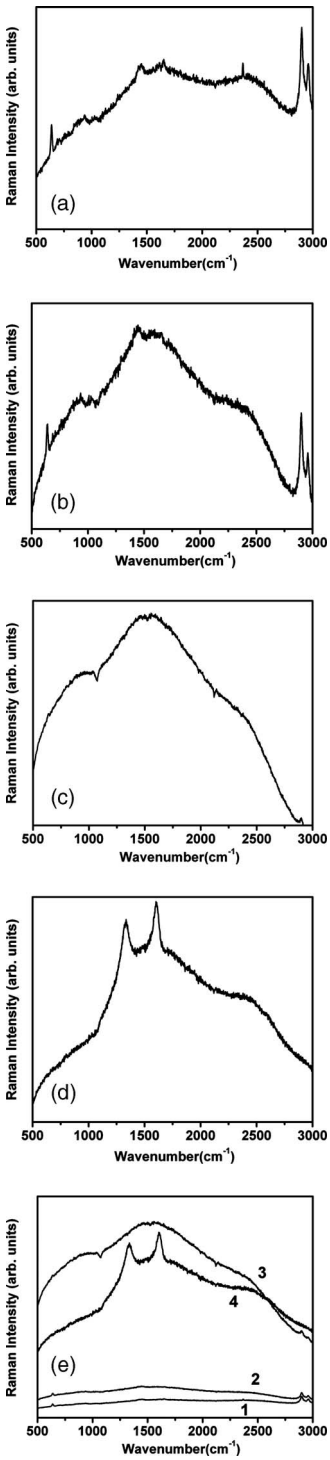

Fig. 6. (a)–(d) Raman spectra of the femtosecond laser modified regions from the periphery (point 1) to the center (point 4) of a damage spot. The acquisition time was 60 s for (a)–(c) and 10 s for (d). (e) shows the relative intensities of the Raman spectra at these four points.

that the Raman signal cannot be separated from the fluorescence. The relative intensity increase of the broad fluorescence band is shown in Fig. 6(e). Thermal decomposition of organic molecules and polymers often contains monomers or other molecule fragments such as polycyclic aromatics that can fluoresce, and we believe that this is the origin of the fluorescent background. Figure 6(d) shows the Raman spectra of the central region of the laser-damaged spot (point 4). One sees peaks for very strong $C-C$ vibrations (D band at $\sim 1330\ \mathrm{cm}^{-1}$, and G band at $\sim 1600\ \mathrm{cm}^{-1}$), together with complete absence of the $C-H$ peaks (at $\sim 3000\ \mathrm{cm}^{-1}$). This is indicative of the pyrolytic decomposition of the polymer matrix to amorphous carbon.

4. DISCUSSION

Different mechanisms have been reported that may contribute to the refractive index changes induced by femtosecond lasers in different materials. It has been proposed that in fused silica glass a shock wave generated by rapid expansion would lead to compression and an increase of refractive index [36], or color centers produced in sufficient numbers and strength would alter the refractive index through a Kramers–Kronig mechanism [37], or structural changes would lead to material density change and modify the refractive index [23,25]. In other doped glasses and polymers it was also proposed that the nanocrystal formation or other densifications may increase the refractive index as well [17,27,38,39].

In these water-swollen silicone-based hydrogel polymers, we hypothesize that the accumulated effect of the femtosecond pulses results in additional localized cross-linking in the polymer network that expels water, causing localized densification of the hydrogel, thereby increasing the local refractive index. Two critical factors that are necessary to yield such observed results are the presence of a significant amount of water inside the material and high-repetition-rate femtosecond pulses.

The presence of water greatly impacts the interaction between the femtosecond laser pulses and the hydrogel polymers below the optical breakdown threshold. Compared with silica glass ($C_P = 840\ \mathrm{J\,K^{-1}\,kg^{-1}}$), water has higher heat capacity ($C_P = 4187\ \mathrm{J\,K^{-1}\,kg^{-1}}$) that could diminish the temperature increase within the nonlinear absorption region at the focus if the same amount of energy was deposited, and eventually increase the heat-induced breakdown threshold. As a result, hydrogel polymers require deposition of more energy before the local temperature becomes high enough to induce thermal damages, if compared with silica glass. Water also has lower heat diffusivity ($k = 1.38 \times 10^{-3}\ \mathrm{cm^2/s}$) than solid silica glass ($k = 8.4 \times 10^{-3}\ \mathrm{cm^2/s}$) yielding lower heat dissipation from the laser–material interaction region into the surrounding medium, and limiting the heat affected zone (HAZ) size. In our experiments, the cross section size of the HAZ was only about $1 \times 3\ \mu\mathrm{m}$ in elliptical shape ($3\ \mu\mathrm{m}$ was the size along the laser beam propagation direction), showing the hydrogel samples have low heat dissipation [10].

Since a 93 MHz femtosecond laser pulse train and a $0.4\ \mu\mathrm{m/s}$ scanning speed was employed to fabricate the refractive index change lines, the laser spot volume was always filled with more than 10^6 pulses. Several research groups have reported that the heat accumulation induced by megahartz femtosecond laser pulses can increase local temperature much more than that caused by kilohertz pulse trains if the pulse energies were the same. Accumulation effects that occur with high repetition rate lasers can induce larger structural modifications and higher re-

fractive index changes in silica glasses [1,2,19,20], and also induce modifications in biomolecules and biomaterials [6,19,21]. To analyze the thermal dynamics of the hydrogel polymer at the laser focus, a heat diffusion model was applied under our experimental conditions [21,40]. We assumed that the energy deposited by the laser pulses is a delta function in time scale since the thermal diffusion time (>0.1 μs) is much longer than the pulse duration (27 fs) and electron heating and electron–phonon coupling time (<1 ps). Then the heat diffusion equation can be written as

$$c_p\rho\frac{\partial}{\partial t}\Delta T(r,t) - k\nabla^2\Delta T(r,t) = 0,$$

where $\Delta T(r,t)$ is the temperature change at a certain point at a distance r away from the laser focus at time t; c_p, ρ, and k are the specific heat, density, and thermal conductivity of the material sample at constant pressure. Since the hydrogel samples contain a significant amount of water, we employed the thermal parameters of pure water in the modeling for simplicity. In the real hydrogel polymers the energy level structure of water may be modified by the polymer network with additional energy levels that may enhance both the linear and nonlinear absorption. The instant temperature increasing by a single laser pulse at the focus can be obtained as $\Delta T(r=0,t=0) = E_a/c_p\rho$, where E_a is the measured absorbed energy density of each pulse in the polymer sample (pulse energy density multiplied by material absorption). Since the hydrogel is transparent at 800 nm and has no absorption under the 800 nm CW laser irradiation, the dominant absorption should be a weak multiphoton absorption that should occur only near the focal region, within the confocal range. We confirmed this by measuring the transmitted light with the hydrogel in and out of focus, and detected a 4.2% decrease of the transmitted pulse energy when the hydrogel was at the focus position. The pulse energy of each femtosecond pulse was 1.3 nJ in our experiments and we assume that 4.2% of it is absorbed within focal volume, as would be expected for multiphoton absorption.

Figure 7 shows the temperature increase evolution of water at the laser focus. Although one single laser pulse can only induce about 18°C temperature increase, the heat accumulation from a 93 MHz pulse train can eventually result in a 150°C temperature increase, which will heat up room-temperature water to about 170°C. Recently, it has been predicted that a threshold temperature of at least 151.5°C is needed to generate nanoscale water bubbles during the femtosecond laser micromachining process in water [21,41]. These theoretical predictions support our previous experimental observations that microscopic water bubbles were formed resulting in enhanced surface roughness of optical waveguides when fabricated by femtosecond laser micromachining in these silicone-based hydrogels [42]. The high repetition rate of the laser pulse train is critical to induce the accumulated heat. Our simulation shows that the temperature evolution of the laser focus with a 10 MHz pulse train results in a 20° increase. It has been reported that 90°C to 200°C is the required temperature range to induce thermal-initiated cross-linkings in the cross-linkable polymers [43]. The cross-linking process will be negligible if the temperature is too low, and the polymers will start to decompose if the temperature is above 250°C [10]. Therefore temperature increase induced by the laser-initiated heat accumulation is sufficient to induce additional cross-linking in the polymer network during the femtosecond laser micromachining process. The cross-linking process alone may change the local refractive index of the polymer [43]. Because of the unique formation of the hydrogels, it may also be possible that the additional thermal-induced cross-linking will cause the expulsion of water, localized densification, and a concomitant increase in the local refractive index. Since the cross-linking polymer component is typically incorporated at the 1% or less level, it would be difficult to detect significant changes in the Raman spectrum in the laser-micromachined regions when the cross-linking polymers are modified, because their Raman signatures may be present at undetectable levels in our noise background. The heat accumulation effects on refractive index changes in hydrogel polymers can also be observed if we change the laser scanning speed. Figure 8 shows the measured refractive index changes within the laser-micromachined region decline from 0.06 to 0.004 when the laser scanning speed was increased from 0.4 μm/s to 50 μm/s while other experimental conditions were kept unchanged. We measured these index changes via differential interference contrast microscope that we calibrated. It is worth noting that that there is no observable damage even if the scanning speed is as slow as 0.4 μm/s, indicating the thermal accumulation from the laser pulse train cannot

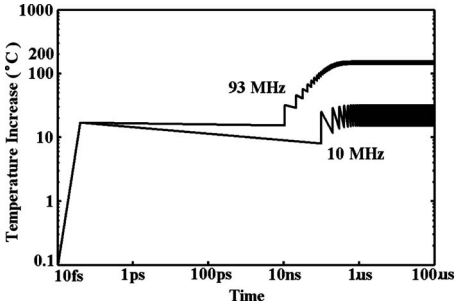

Fig. 7. Temperature increase at the laser focus induced by 800 nm, 27 fs laser pulses in water. The 93 MHz pulse train used in our experiment can create as high as a 150°C temperature increase. In the contrast, a 10 MHz pulse train can only provide about a 20°C temperature increase at the laser focus.

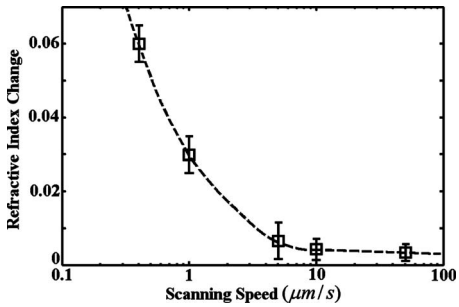

Fig. 8. Refractive index changes of the hydrogel polymers as a function of laser scanning speed.

raise the temperature enough to induce damage while it can still induce large refractive index changes in the hydrogel polymer. In fact, the irradiance conditions in our case were below the optical breakdown threshold of the hydrogel polymers, and the femtosecond laser pulses could at most generate a low-density plasma while not yielding high temperature increase and visible plasma luminescence [21].

To check the model proposed here, we further reproduced a similar experiment using dry Balafilcon A elastomer samples containing no water. The heat accumulation increased the local temperature promptly, and gross damage and burning in the polymer was observed with significantly lower optical powers. Figure 9(a) shows a phase contrast image of several damage lines micromachined by femtosecond laser pulses 200 μm below the top surface within one dry Balafilcon A elastomer sample. The same-laser exposure parameters such as 1.3 nJ pulse energy, 93 MHz repetition rate, 800 nm wavelength, 27 fs pulse duration, and 0.70 NA focusing were employed. Instead of the 0.4 μm/s scanning speed, which was used for hydrogel polymers, a much faster scanning speed of 50 μm/s was used to avoid burning and gross damages induced by laser-initiated heat accumulation in the elastomer. However shining visible plasma luminescence was still observed during the micromachining process, indicating the laser pulse train could induce much a higher temperature increase and generate a high-density visible microplasma. The discontinuous damage spots along these lines can be easily observed under a bright field microscope [Fig. 9(b)] indicating they are not pure refractive index change. There is no obvious refractive index change region among the damage spots along these lines as shown in the phase contrast image [Fig. 9(a)]. These results indicate that observable refractive index changes are difficult to induce in the polymer network without water. Similar results were also observed even when much lower laser exposure was employed.

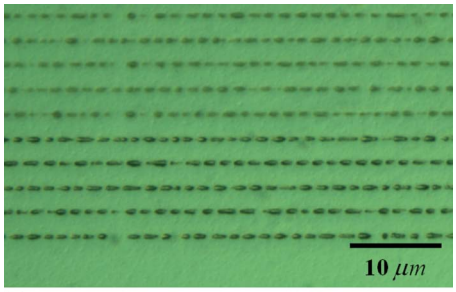

(a)

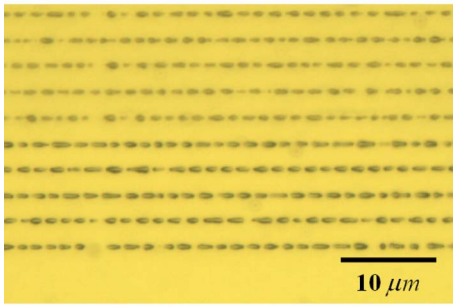

(b)

Fig. 9. (Color online) (a) Phase contrast image of damage lines micromachined by the femtosecond laser pulses inside a Balafilcon A elastomer sample containing no water. The same laser exposure conditions were employed, but the scanning speed was set to be much faster (50 μm/s) to avoid gross damages and burning. (b) Bright field image of the damaged lines.

5. CONCLUSION

Micro-Raman spectroscopic method and a thermal model were employed to study the modifications induced by high-repetition-rate, low-pulse-energy femtosecond laser pulses in ophthalmologic silicone-based hydrogel polymers. No significant changes in characteristic Raman peaks and background fluorescence were detected, below the optical breakdown threshold, even when the refractive index change was up to +0.06. Comparative Raman spectra and background fluorescence on femtosecond laser damaged spots were also obtained. The comparative Raman spectra prove that the refractive index modifications below the optical breakdown threshold were not accompanied by significant change in the structure of the polymer matrix. From the thermal model, we ascertain that accumulated thermal heat from the nonlinear absorption of the femtosecond laser pulses resulted in additional cross-linking of the polymer matrix, expulsion of water molecules from the hydrogel, local densification of the polymer matrix, and substantial change of the refractive index. The accumulated heat may also be responsible for the increase of the fluorescence background in different femtosecond laser modified regions.

ACKNOWLEDGMENTS

This research work was supported by grants from Bausch and Lomb, Inc. and the Center for Electronic Imaging Systems (CEIS) program 0833810 at the University of Rochester, and was also partially supported by the U.S. Department of Energy (DOE) through grant DE-FG02-05ER46207. We thank Thomas Smith from Rochester Institute of Technology for helpful discussions.

REFERENCES

1. K. M. Davis, K. Miura, N. Sugimoto, and K. Hirao, "Writing waveguides in glass with a femtosecond laser," Opt. Lett. **21**, 1729–1731 (1996).
2. D. Homoelle, S. Wielandy, A. L. Gaeta, N. F. Borrelli, and C. Smith, "Infrared photosensitivity in silica glasses exposed to femtosecond laser pulses," Opt. Lett. **24**, 1311–1313 (1999).
3. A. M. Streltsov and N. F. Borrelli, "Fabrication and analysis of a directional coupler written in glass by nanojoule femtosecond laser pulses," Opt. Lett. **26**, 42–43 (2001).
4. C. B. Schaffer, A. Brodeur, J. F. Garcia, and E. Mazur, "Micromachining bulk glass by use of femtosecond laser pulses with nanojoule energy," Opt. Lett. **26**, 93–95 (2001).
5. K. Minoshima, A. M. Kowalevicz, I. Hartl, E. P. Ippen, and J. G. Fujimoto, "Photonic device fabrication in glass by use of nonlinear materials processing with a femtosecond laser oscillator," Opt. Lett. **26**, 1516–1518 (2001).
6. S. M. Eaton, H. Zhang, P. R. Herman, F. Yoshino, L. Shah, J. Bovatsek, and A. Y. Arai, "Heat accumulation effects in femtosecond laser-written waveguides with variable repetition rate," Opt. Express **13**, 4708–4716 (2005).

7. E. N. Glezer, M. Milosavljevic, L. Huang, R. J. Finlay, T. H. Her, J. P. Callan, and E. Mazur, "Three-dimensional optical storage inside transparent materials," Opt. Lett. **21**, 2023–2025 (1996).
8. Y. Li, K. Itoh, W. Watanabe, K. Yamada, D. Kuroda, J. Nishii, and Y. Jiang, "Three-dimensional hole drilling of silica glass from the rear surface with femtosecond laser pulses," Opt. Lett. **26**, 1912–1914 (2001).
9. D. J. Hwang, T. Y. Choi, and C. P. Grigoropoulos, "Liquid-assisted femtosecond laser drilling of straight and three-dimensional microchannels in glass," Appl. Phys. A **79**, 605–612 (2004).
10. L. Ding, R. Blackwell, J. F. Künzler, and W. H. Knox, "Large refractive index change in silicone-based and non-silicone-based hydrogel polymers induced by femtosecond laser micromachining," Opt. Express **14**, 11901–11909 (2006).
11. S. Maruo, O. Nakamura, and S. Kawata, "Three-dimensional microfabrication with two-photon-absorbed photopolymerization," Opt. Lett. **22**, 132–134 (1997).
12. G. Witzgall, R. Vrigen, E. Yablonovitch, V. Doan, and B. J. Schwartz, "Single-shot two-photon exposure of commercial photoresist for the production of three-dimensional structures," Opt. Lett. **23**, 1745–1747 (1998).
13. A. Zoubir, C. Lopez, M. Richardson, and K. Richardson, "Femtosecond laser fabrication of tubular waveguides in poly(methyl methacrylate)," Opt. Lett. **29**, 1840–1842 (2004).
14. S. Sowa, W. Watanabe, T. Tamaki, J. Nishii, and K. Itoh, "Symmetric waveguides in poly(methyl methacrylate) fabricated by femtosecond laser pulses," Opt. Express **14**, 291–297 (2006).
15. G. Zhou, M. J. Ventura, M. R. Vanner, and M. Gu, "Use of ultrafast-laser-driven microexplosion for fabricating three-dimensional void-based diamond-lattice photonic crystals in a solid polymer material," Opt. Lett. **29**, 2240–2242 (2004).
16. D. Day and M. Gu, "Microchannel fabrication in PMMA based on localized heating by nanojoule high repetition rate femtosecond pulses," Opt. Express **13**, 5939–5946 (2005).
17. C. R. Mendonca, L. R. Cerami, T. Shih, R. W. Tilghman, T. Baldacchini, and E. Mazur, "Femtosecond laser waveguide micromachining of PMMA films with azoaromatic chromophores," Opt. Express **16**, 200–206 (2008).
18. C. C. S. Karlgard, D. K. Sarkar, L. W. Jones, C. Moresoli, and K. T. Leung, "Drying methods for XPS analysis of PureVision™, Focus® Night&Day™ and conventional hydrogel contact lens," Appl. Surf. Sci. **230**, 106–114 (2004).
19. C. B. Schaffer, J. F. Garcia, and E. Mazur, "Bulk heating of transparent materials using a high-repetition-rate femtosecond laser," Appl. Phys. A **76**, 351–354 (2003).
20. A. M. Streltsov and N. F. Borrelli, "Study of femtosecond-laser-written waveguides in glasses," J. Opt. Soc. Am. B **19**, 2496–2504 (2002).
21. A. Vogel, J. Noack, G. Huttman, and G. Paltauf, "Mechanisms of femtosecond laser nanosurgery of cells and tissues," Appl. Phys. B **81**, 1015–1047 (2005).
22. C. B. Schaffer, N. Nishimura, E. N. Glezer, A. Kim, and E. Mazur, "Dynamic of femtosecond laser-induced breakdown in water from femtoseconds to microseconds," Opt. Express **10**, 196–203 (2002).
23. J. W. Chan, T. Huser, S. Risbud, and D. M. Krol, "Structural changes in fused silica after exposure to focused femtosecond laser pulses," Opt. Lett. **26**, 1726–1728 (2001).
24. J. W. Chan, T. R. Huser, S. H. Risbud, and D. M. Krol, "Modification of the fused silica glass network associated with waveguide fabrication using femtosecond laser pulses," Appl. Phys. A **76**, 367–372 (2003).
25. W. J. Reichman, D. M. Krol, L. Shah, F. Yoshino, A. Arai, S. M. Eaton, and P. R. Herman, "A spectroscopic comparison of femtosecond-laser-modified fused silica using kilohertz and megahertz laser systems," J. Appl. Phys. **99**, 123112 (2006).
26. B. Yu, B. Chen, X. Y. Yang, J. R. Qiu, X. W. Jiang, C. S. Zhu, and K. Hirao, "Study of crystal formation in borate, niobate, and titanate glasses irradiated by femtosecond laser pulses," J. Opt. Soc. Am. B **21**, 83–87 (2004).
27. D. K. Y. Low, H. Xie, Z. Xiong, and G. C. Lim, "Femtosecond laser direct writing of embedded optical waveguides in aluminosilicate glass," Appl. Phys. A **81**, 1633–1638 (2005).
28. B. Zhu, Y. Dai, H. Ma, S. Zhang, G. Lin, and J. Qiu, "Femtosecond laser induced space-selective precipitation of nonlinear optical crystals in rare-earth-doped glasses," Opt. Express **15**, 6069–6074 (2007).
29. M. S. Amer, M. A. El-Ashry, L. R. Dosser, K. E. Hix, J. F. Maguire, and B. Irwin, "Femtosecond versus nanosecond laser machining: comparison of induced stresses and structural changes in silicon wafers," Appl. Surf. Sci. **242**, 162–167 (2005).
30. G. J. Lee, J. Park, E. K. Kim, Y. P. Lee, K. M. Kim, H. Cheong, C. S. Yoon, Y. D. Son, and J. Jang, "Microstructure of femtosecond laser-induced grating in amorphous silicon," Opt. Express **13**, 6445–6453 (2005).
31. A. Zoubir, M. Richardson, C. Rivero, A. Schulte, C. Lopez, K. Richardson, N. Ho, and R. Valle, "Direct femtosecond laser writing of waveguides in As_2S_3 thin films," Opt. Lett. **29**, 748–750 (2004).
32. S. Kuper, S. Modaressi, and M. Stuke, "Photofragmentation pathways of a PMMA model-compound under UV excimer laser ablation conditions," J. Phys. Chem. **94**, 7514–7518 (1990).
33. A. Baum, P. J. Scully, M. Basanta, C. L. P. Thomas, P. R. Fielden, N. J. Goddard, W. Perrie, and P. R. Chalker, "Photochemistry of refractive index structures in poly(methyl methacrylate) by femtosecond laser irradiation," Opt. Lett. **32**, 190–192 (2007).
34. D. Lin-Vien, N. B. Colthup, W. G. Fateley, and J. G. Grasselli, *The Handbook of Infrared and Raman Characteristic Frequencies of Organic Molecules* (Academic, 1991).
35. G. Socrates, *Infrared Characteristic Group Frequencies* (Wiley, 1997).
36. C. B. Schaffer, A. Brodeur, and E. Mazur, "Laser-induced breakdown and damage in bulk transparent materials induced by tightly focused femtosecond laser pulses," Meas. Sci. Technol. **12**, 1784–1794 (2001).
37. K. Hirao and K. Miura, "Writing waveguides and gratings in silica and related materials by a femtosecond laser," J. Non-Cryst. Solids **239**, 91–95 (1998).
38. N. Takeshima, Y. Kuroiwa, Y. Narita, S. Tanaka, and K. Hirao, "Fabrication of a periodic structure with a high refractive-index difference by femtosecond laser pulses," Opt. Express **12**, 4019–4024 (2004).
39. N. Takeshima, Y. Narita, S. Tanaka, Y. Kuroiwa, and K. Hirao, "Fabrication of high-efficiency diffraction gratings in glass," Opt. Lett. **30**, 352–354 (2005).
40. Y. Jaluria and K. E. Torrance, *Computational Heat Transfer* (Taylor & Francis, 2003).
41. A. Vogel, N. Linz, S. Freidank, and G. Paltauf, "Femtosecond-laser-induced nanocavitation in water: implications for optical breakdown threshold and cell surgery," Phys. Rev. Lett. **100**, 038102 (2008).
42. L. Ding, R. I. Blackwell, J. F. Kunzler, and W. H. Knox, "Femtosecond laser micromachining of waveguides in silicone-based hydrogel polymers," Appl. Opt. **47**, 3100–3108 (2008).
43. J. S. Koo, P. G. R. Smith, R. B. Williams, C. Riziotis, and M. C. Grossel, "UV written waveguides using crosslinkable PMMA-based copolymers," Opt. Mater. **23**, 583–592 (2003).